

# A Functional Interpretation of Gravitational Inaccessibility: The Hypothesis of Vibrational Wave Dispersion (HDOV)

Arnoldo Walter Fernández  
arnoldo@unsj.edu.ar

July 5, 2025

Version 5.3 — referee-oriented revision

## Abstract

We present a revised version of the HDOV formalism (Hypothesis of Vibrational Wave Dispersion), focused on its minimal gravitational sector. The core of the model is organized into three complementary levels: a projective wave equation for the scalar field  $\Psi$ , a WKB transport law for its amplitude, and a minimal geometric closure for the functional parameter  $\eta_p$ . In this version, that closure is adopted as a leading covariant ansatz,  $\eta_p = \xi R$ , motivated by an EFT truncation in curvature; as a result, the interferometric visibility derived from the amplitude is no longer a free parametrization, but becomes dependent on the background geometry. On this basis we explicitly derive the minimal metric sector associated with the coupling  $\lambda R X$ , obtaining the effective field equations, their trace, the reduction to an FLRW background, and the linear limit relevant for the post-Newtonian sector. We show that, in the vacuum branch with  $\bar{\Psi} = 0$ , the scalar field is not sourced by ordinary matter at first order and the PPN sector coincides with General Relativity, with  $\gamma = \beta = 1$ . For slowly varying homogeneous backgrounds, the leading effect is a renormalization of  $G_{\text{eff}}$  without gravitational slip at linear order. The comparison with Type Ia Supernovae (Pantheon) and BAO (SDSS DR16) is reframed in this version as a reproducible phenomenological benchmark: its figures and metrics diagnose an effective parametrization compatible with HDOV, but they do not replace the self-consistent dynamical solution of the FLRW system. We also make explicit the minimal cosmological extension with matter and radiation, which is required to move from an idealized scalar branch to a dynamical validation. Finally, EFT conditions and minimal stability criteria are formulated to delimit the perturbative domain of the truncation. The purpose of the manuscript is to provide a self-contained, falsifiable, and mathematically more closed formulation of the gravitational sector of HDOV, while explicitly separating derived results, closure ansätze, and the pending observational program.

# Contents

<b>1</b>	<b>Introduction</b>	<b>3</b>
<b>2</b>	<b>Foundations of the HDOV Framework</b>	<b>3</b>
2.1	Motivation from Effective Field Theory . . . . .	3
2.2	Action and Projective Wave Equation . . . . .	4
2.3	WKB Transport and Dimensionally Unambiguous Attenuation Law . . . . .	4
2.4	Normalization, Dimensions and Notation . . . . .	4
2.5	Operational Interpretation of the GFoV . . . . .	5
2.6	Conservation Check in the Classical Limit . . . . .	6
<b>3</b>	<b>Derived Accessibility Magnitude</b>	<b>6</b>
<b>4</b>	<b>Minimal Metric Sector of HDOV</b>	<b>7</b>
4.1	Relation to Horndeski and EFT Character of the Geometric Coupling . . . . .	8
4.2	Homogeneous Cosmological Background and Rolling Branch . . . . .	9
4.3	Inclusion of Matter, Radiation, and Minimal Cosmological Closure . . . . .	9
4.4	EFT Conditions and Minimal Stability of the Truncation . . . . .	10
<b>5</b>	<b>Linear Limit and Post-Newtonian Sector</b>	<b>12</b>
5.1	Post-Newtonian Counting and Local Vacuum Branch . . . . .	13
5.2	Slowly Varying Homogeneous Background and Effective Gravitational Constant . . . . .	13
5.3	Possible Sources of PPN Deviations . . . . .	14
5.4	Scope of the PPN Result . . . . .	15
<b>6</b>	<b>Reproducible Phenomenological Benchmark with SN Ia and BAO</b>	<b>15</b>
6.1	Operational Definition of the Benchmark . . . . .	16
6.2	Phenomenological Figures and Residuals . . . . .	16
6.3	Effective Expansion History and Interpretation of the Closure . . . . .	19
6.4	Diagnostic Metrics and Statistical Scope . . . . .	19
<b>7</b>	<b>Discussion and Conclusions</b>	<b>21</b>
7.1	HDOV in the Context of Other Theoretical Models . . . . .	21
7.2	Regime of Effective Validity and Consistency . . . . .	22
7.3	Limitations and Future Directions . . . . .	22
7.4	Predictions and Falsifiability Criteria in the Regime Considered . . . . .	22
<b>A</b>	<b>EFT Motivation for the Minimal Closure</b>	<b>23</b>
<b>B</b>	<b>Sketch of the Metric Variation of the Geometric Coupling</b>	<b>23</b>

# 1 Introduction

The HDOV hypothesis proposes a geometry-dependent functional projection mechanism that modulates the *accessibility* of degrees of freedom. Motivated by tensions between General Relativity and Quantum Mechanics in high-curvature regimes, HDOV suggests that part of what we interpret as *inaccessibility* or *manifestation* (for example, effective expansions) may arise from a dynamical coarse-graining over an effective medium. In this picture, microscopic information becomes inaccessible to a macroscopic measuring agent, not because it is destroyed, but because it is dispersed into degrees of freedom that are not operationally measurable. The focus of this work is a minimal, testable formulation compatible with standard quantitative tests (Almheiri et al., 2013).

In this revision we adopt a more precise goal: to isolate a minimal gravitational sector, fix a leading geometric closure for  $\eta_p$ , make the associated metric response explicit, and develop the linear limit relevant to the post-Newtonian sector. The comparison with cosmological data is presented here as a reproducible phenomenological benchmark compatible with the formalism, while strong-gravity tests and a self-consistent FLRW validation remain open problems requiring additional development of the metric sector. In particular, the modified wave equation fixes how  $\Psi$  propagates once the functional modulation is specified, but it does not determine by itself the form of  $\eta_p$ ; therefore, the closure  $\eta_p = \xi R$  must be understood in this work as a minimal covariant ansatz, not as a complete microscopic derivation nor as an exclusion of other possible EFT operators.

## 2 Foundations of the HDOV Framework

This section introduces the mathematical core of the HDOV hypothesis. The starting point is an effective action describing a scalar field non-minimally coupled to gravity, which leads to a modified wave equation.

### 2.1 Motivation from Effective Field Theory

The introduction of the projection parameter  $\eta_p$  is motivated by effective field theory in curved spacetime (Birrell and Davies, 1982; Parker and Toms, 2009; Horndeski, 1974; Kobayashi et al., 2011; Bellini and Sawicki, 2014). The modified wave equation determines how a given modulation affects the propagation of  $\Psi$ , but it does not by itself fix the functional form of  $\eta_p$ ; therefore, an additional constitutive relation is required to close the model. Rather than leaving this sector undetermined, we adopt here a minimal covariant gravitational ansatz. The word *ansatz* is important: in this version we do not claim to derive the closure  $\eta_p = \xi R$  microscopically, but select the simplest local curvature operator that makes the truncation calculable. As a dimensional and covariant guide, the schematic effective starting point can be written as

$$\Gamma_{\text{eff}} = \Gamma_{\text{EH}} + \Gamma_{\text{matter}} + \Gamma_{\text{non-local}} + \dots \quad (1)$$

where  $\Gamma_{\text{non-local}}$  schematically summarizes quantum-memory corrections depending on causal history. At leading order in a local low-curvature expansion, a minimal covariant choice is to take a coupling proportional to  $R/M^2$ . In this manuscript we adopt precisely that operator as the operative closure of the gravitational sector,

$$\eta_p(x) = \xi R(x), \quad \xi \equiv \alpha/M^2, \quad (2)$$

reserving non-local terms and higher-order corrections for future developments. Other invariants, such as  $R^2$ ,  $R_{\mu\nu}R^{\mu\nu}$ ,  $R_{\mu\nu\rho\sigma}R^{\mu\nu\rho\sigma}$ ,  $\square R$ , or non-local combinations, are also compatible with a more general gravitational EFT. They are omitted here by the decision to work with a minimal truncation, not because they have been dynamically or observationally ruled out.

## 2.2 Action and Projective Wave Equation

The dynamics of the system is derived from the following action, which includes an explicit coupling between the scalar field  $\Psi$  and the geometry, mediated by an auxiliary field  $\chi(I)$ :

$$S = \int d^4x \sqrt{-g} \left[ \frac{1}{2} (1 + 2g_c \chi(I)) g^{\mu\nu} \partial_\mu \Psi \partial_\nu \Psi - \frac{1}{2} m^2 \Psi^2 + \frac{1}{2} g^{\mu\nu} \partial_\mu \chi(I) \partial_\nu \chi(I) - V(\chi(I)) \right]. \quad (3)$$

The action in Eq. (3) should be read as a low-energy effective action inspired by decoherence and stochastic-gravity mechanisms (Bassi and Ghirardi, 2003; Hu and Verdaguer, 2004), not as a unique reconstruction of a microscopic theory. Varying this action with respect to  $\Psi$ , and treating the coupling term as a functional parameter  $\eta_p \equiv \chi(I)$ , gives the projective wave equation

$$\nabla_\mu [(1 + 2g_c \eta_p) \nabla^\mu \Psi] + m^2 \Psi = 0. \quad (4)$$

Although the general action includes an independent dynamics for the auxiliary field  $\chi$ , in the present minimal version we do not solve that sector independently. Instead, we work with the geometric closure of Eq. (2), so that the projective equation is fully specified at leading order by the scalar curvature of the background. This choice should be read as a low-energy effective truncation: it makes the model calculable and reduces phenomenological arbitrariness, but it does not replace a first-principles derivation of the full auxiliary sector.

## 2.3 WKB Transport and Dimensionally Unambiguous Attenuation Law

In the eikonal regime,  $\Psi = A e^{i\Theta}$  with  $k_\mu = \nabla_\mu \Theta$  and  $k^\mu \nabla_\mu \equiv d/d\lambda$ . Starting from  $\nabla_\mu [(1 + 2g_c \eta_p) \nabla^\mu \Psi] = 0$  and separating orders in the WKB expansion, the amplitude transport equation is

$$\frac{d \ln A}{d\lambda} = -\frac{1}{2} \theta - \frac{1}{2} \frac{d}{d\lambda} \ln(1 + 2g_c \eta_p), \quad \theta \equiv \nabla_\mu k^\mu. \quad (5)$$

For  $|2g_c \eta_p| \ll 1$ ,

$$\frac{d \ln A}{d\lambda} \simeq -\frac{1}{2} \theta - g_c \frac{d\eta_p}{d\lambda}. \quad (6)$$

Integrating along the ray between  $\lambda_0$  and  $\lambda$  gives

$$\ln \frac{A(\lambda)}{A(\lambda_0)} = -\frac{1}{2} \int_{\lambda_0}^{\lambda} \theta d\lambda' - \frac{1}{2} \ln \frac{1 + 2g_c \eta_p(\lambda)}{1 + 2g_c \eta_p(\lambda_0)} \simeq -\frac{1}{2} \int_{\lambda_0}^{\lambda} \theta d\lambda' - g_c [\eta_p(\lambda) - \eta_p(\lambda_0)]. \quad (7)$$

Equation (7) is dimensionless and does not require introducing a length-scale constant: the geometric term ( $\theta$ ) and the functional variation of  $\eta_p$  play distinct and compatible roles.

## 2.4 Normalization, Dimensions and Notation

To avoid notational collisions, we distinguish: (i)  $g \equiv \det(g_{\mu\nu})$  (only inside  $\sqrt{-g}$ ) and (ii)  $g_c$  as the dimensionless coupling constant multiplying  $\eta_p$  in the effective kinetic term.

**Dimensions and consistency of the action.** We work in natural units  $\hbar = c = 1$ , where the action is dimensionless and the Lagrangian density has mass dimension four. For a scalar  $\Psi$  with dimension  $[\Psi] = \text{mass}$ , the standard kinetic term  $\frac{1}{2} g^{\mu\nu} \partial_\mu \Psi \partial_\nu \Psi$  already has the correct dimension. Therefore, the multiplicative factor  $(1 + 2g_c \eta_p)$  modulating the kinetic term must be dimensionless. We thus require both  $g_c$  and  $\eta_p$  to be dimensionless. In particular, if  $\eta_p = \xi R$ , dimensional consistency requires  $[\xi] = \text{mass}^{-2}$ , justifying the notation  $\xi = \alpha/M^2$  with dimensionless  $\alpha$ . With this convention, the projective wave equation used in the text,

$$\nabla_\mu [(1 + 2g_c \eta_p) \nabla^\mu \Psi] + m^2 \Psi = 0, \quad (8)$$

is dimensionally consistent.

**Notation.** We use  $\eta_p$  for the functional parameter that modulates the projective wave equation, and  $\mathcal{V}_p$  for the interferometric visibility derived from the amplitude. These quantities do not represent the same object:  $\eta_p$  enters as an effective geometric modulation of the dynamics, while  $\mathcal{V}_p$  is obtained a posteriori from the WKB transport law. Once the geometric closure for  $\eta_p$  has been fixed,  $\mathcal{V}_p$  is no longer a free parametrization but a derived quantity.

**Parameters and physical regime.** For physical auditability, Table 1 summarizes the main effective quantities of the minimal truncation. The observable combination relevant to the metric sector is  $\lambda = g_c \xi$ , whereas  $\eta_p$  and  $\mathcal{V}_p$  play conceptually different roles: the former modulates the dynamics and the latter quantifies the propagative effect on the amplitude.

**Table 1:** Main parameters of the minimal metric truncation of HDOV. The table summarizes the dimension of each quantity, its physical role in the model, and the validity regime assumed in the manuscript; the listed conditions are working assumptions of the effective truncation, not results of global stability.

Parameter	Dimension	Physical role	Assumed regime
$g_c$	dimensionless	functional coupling	$ g_c \eta_p  \ll 1$ in perturbative WKB
$\xi$	$\text{mass}^{-2}$	geometric closure $\eta_p = \xi R$	leading EFT in curvature
$\lambda = g_c \xi$	$\text{mass}^{-2}$	metric coupling $\lambda R X$	$ 2\lambda R  \ll 1$
$m$	mass	scalar-field scale	free, to be fixed phenomenologically
$\eta_p$	dimensionless	effective geometric modulation	derived from the adopted closure
$\mathcal{V}_p$	dimensionless	visibility derived from the amplitude	not free once $\eta_p$ is fixed

## 2.5 Operational Interpretation of the GFoV

We introduce the notion of a Gravitational Field of View (GFoV) as an operational interpretation of the regime in which the functional modulation effectively suppresses certain modes from the accessible subspace. At this stage, the threshold  $\eta_\star$  should be understood as a phenomenological value rather than as a derived universal constant. Figure 1 therefore plays a strictly conceptual role.

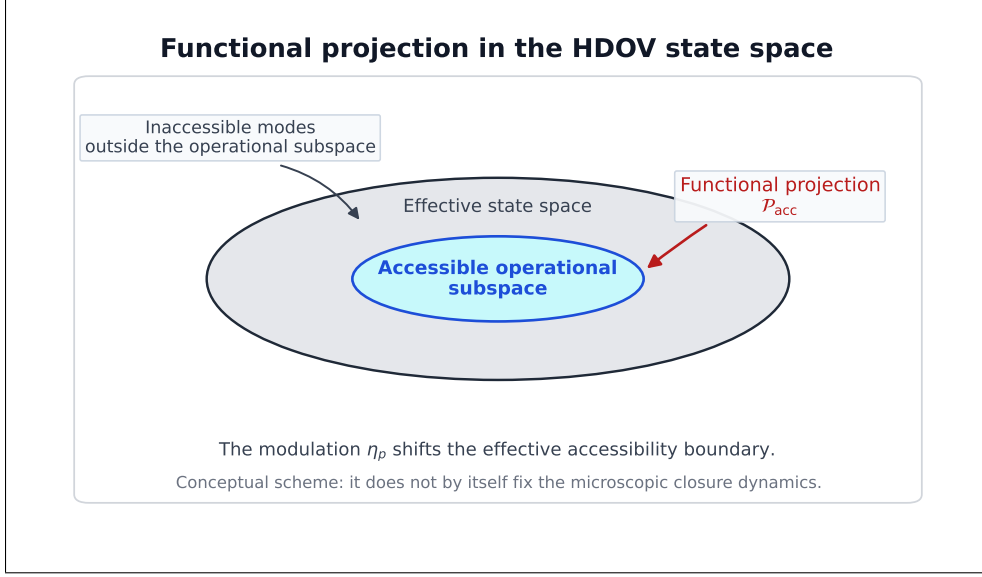


**Figure 1:** Conceptual scheme of functional projection in HDOV. The outer region represents the effective state space, the inner region the accessible operational subspace, and the arrow indicates the idealized action of the functional projector on the relevant modes. The figure illustrates the operational interpretation of the GFoV and does not represent a simulation or a microscopic derivation of the geometric closure.

## 2.6 Conservation Check in the Classical Limit

In the minimal formulation, the Bianchi identity guarantees the covariant conservation of the geometric side once the HDOV sector is included in the metric system. In the classical limit  $\eta_p \rightarrow 0$ , the additional sector switches off and the standard conservation law is recovered. Beyond that limit, covariant consistency depends on the field equations derived in Section 4.

## 3 Derived Accessibility Magnitude

The WKB law obtained in Section 2.3 allows us to define the interferometric visibility

$$\mathcal{V}_p(\lambda) \equiv \frac{|A(\lambda)|^2}{|A(\lambda_0)|^2}, \quad (9)$$

which must not be confused with the functional parameter  $\eta_p$  introduced in the projective equation. Separating the purely GR geometric focusing, the HDOV contribution can be written as

$$\mathcal{V}_p(\lambda) = \exp[-2g_c(\eta_p(\lambda) - \eta_p(\lambda_0))] \equiv \exp[-2u(\lambda)], \quad (10)$$

with

$$u(\lambda) \equiv g_c[\eta_p(\lambda) - \eta_p(\lambda_0)]. \quad (11)$$

Once the minimal closure  $\eta_p = \xi R$  is fixed,  $\mathcal{V}_p$  ceases to be a free parametrization and becomes a geometry-derived quantity. In cosmology,

$$\mathcal{V}_p(z) = \exp[-2g_c\xi(R(z) - R_0)], \quad (12)$$

where  $R_0$  is the scalar curvature at the chosen reference point. This relation provides the conceptual bridge between the metric sector and the later phenomenological exploration. In this hierarchy,  $\eta_p$  acts as the geometric input of the model, whereas  $\mathcal{V}_p$  quantifies its propagative effect on the amplitude.

## 4 Minimal Metric Sector of HDOV

A central technical gap in previous versions of the manuscript was the absence of an explicit metric variation. If the leading closure

$$\eta_p(x) = \xi R(x), \quad \xi \equiv \alpha/M^2, \quad (13)$$

is adopted, the effective kinetic term can be rewritten as

$$\frac{1}{2}(1 + 2g_c\eta_p)\nabla_\mu\Psi\nabla^\mu\Psi = \frac{1}{2}X + \lambda RX, \quad X \equiv \nabla_\mu\Psi\nabla^\mu\Psi, \quad \lambda \equiv g_c\xi. \quad (14)$$

This leads to the minimal metric action

$$S[g, \Psi] = \int d^4x \sqrt{-g} \left[ \frac{1}{2\kappa}R + \frac{1}{2}X - \frac{1}{2}m^2\Psi^2 + \lambda RX \right], \quad (15)$$

where  $\kappa \equiv 8\pi G$ .

Variation with respect to the scalar field gives

$$\nabla_\mu [(1 + 2\lambda R)\nabla^\mu\Psi] + m^2\Psi = 0, \quad (16)$$

which coincides with the original projective equation after identifying  $\eta_p = \xi R$ .

To make the metric variation of the term  $\lambda RX$  explicit, we vary with respect to the inverse metric  $g^{\mu\nu}$  and use

$$\delta X = \nabla_\mu\Psi\nabla_\nu\Psi\delta g^{\mu\nu}, \quad \delta(\sqrt{-g}R) = \sqrt{-g}[G_{\mu\nu}\delta g^{\mu\nu} + (g_{\mu\nu}\square - \nabla_\mu\nabla_\nu)\delta g^{\mu\nu}], \quad (17)$$

with boundary terms integrated by parts. With these conventions, the direct variation of

$$S_\lambda = \int d^4x \sqrt{-g} \lambda RX \quad (18)$$

is determined by the tensorial block

$$\mathcal{A}_{\mu\nu}^{(\lambda)} \equiv XG_{\mu\nu} + (g_{\mu\nu}\square - \nabla_\mu\nabla_\nu)X + R\nabla_\mu\Psi\nabla_\nu\Psi, \quad (19)$$

so that

$$\delta S_\lambda = \int d^4x \sqrt{-g} \lambda \mathcal{A}_{\mu\nu}^{(\lambda)} \delta g^{\mu\nu}, \quad (20)$$

up to total divergences. The sign of the last term in the effective field equations should not be read directly from Eq. (20), but from the contribution that this block induces on the right-hand side of the metric equations. With the convention used in this manuscript,  $G_{\mu\nu} = \kappa T_{\mu\nu}^{\text{eff}}$ , that contribution is  $-2\lambda\mathcal{A}_{\mu\nu}^{(\lambda)}$ .

Defining

$$T_{\mu\nu}^{(0)} = \nabla_\mu\Psi\nabla_\nu\Psi - g_{\mu\nu}\left(\frac{1}{2}X - \frac{1}{2}m^2\Psi^2\right), \quad (21)$$

the metric equation can first be written as

$$\frac{1}{\kappa}G_{\mu\nu} = T_{\mu\nu}^{(0)} - 2\lambda\mathcal{A}_{\mu\nu}^{(\lambda)}. \quad (22)$$

Substituting the definition of  $\mathcal{A}_{\mu\nu}^{(\lambda)}$  and moving the term proportional to  $XG_{\mu\nu}$  to the left-hand side gives the operative form

$$\left(\frac{1}{\kappa} + 2\lambda X\right)G_{\mu\nu} = T_{\mu\nu}^{(0)} + 2\lambda(\nabla_\mu\nabla_\nu - g_{\mu\nu}\square)X - 2\lambda R\nabla_\mu\Psi\nabla_\nu\Psi. \quad (23)$$

This is the form used throughout the paper. Equivalently,

$$G_{\mu\nu} = \kappa \left( T_{\mu\nu}^{(0)} + T_{\mu\nu}^{\text{HDOV}} \right), \quad (24)$$

with

$$T_{\mu\nu}^{\text{HDOV}} = \frac{2\lambda}{1 + 2\kappa\lambda X} [(\nabla_\mu \nabla_\nu - g_{\mu\nu} \square) X - R \nabla_\mu \Psi \nabla_\nu \Psi - X G_{\mu\nu}]. \quad (25)$$

This compact form is obtained by solving for  $T_{\mu\nu}^{\text{HDOV}}$  in Eq. (23) after regrouping the terms. The covariant conservation of the full system is understood in the usual sense of a diffeomorphism-invariant action:  $T_{\mu\nu}^{\text{HDOV}}$  need not be separately conserved off shell, but the full right-hand side is compatible with the Bianchi identity when the equations of motion are satisfied.

Taking the trace of Eq. (23) gives

$$R = \kappa \left( X - 2m^2 \Psi^2 + 6\lambda \square X \right). \quad (26)$$

In a spatially flat FLRW background with  $\Psi = \Psi(t)$  and  $R = 6(\dot{H} + 2H^2)$ , the scalar equation reduces to

$$(1 + 2\lambda R)(\ddot{\Psi} + 3H\dot{\Psi}) + 2\lambda \dot{R}\dot{\Psi} + m^2 \Psi = 0, \quad (27)$$

whereas the background equations take the form

$$3H^2 \left( \frac{1}{\kappa} + 2\lambda \dot{\Psi}^2 \right) = \rho_\Psi - 6\lambda H \dot{X} - 2\lambda R \dot{\Psi}^2, \quad (28)$$

$$-(2\dot{H} + 3H^2) \left( \frac{1}{\kappa} + 2\lambda \dot{\Psi}^2 \right) = p_\Psi - 2\lambda (\ddot{X} + 2H\dot{X}), \quad (29)$$

with  $\rho_\Psi = \frac{1}{2}\dot{\Psi}^2 + \frac{1}{2}m^2\Psi^2$  and  $p_\Psi = \frac{1}{2}\dot{\Psi}^2 - \frac{1}{2}m^2\Psi^2$ .

#### 4.1 Relation to Horndeski and EFT Character of the Geometric Coupling

The operator  $\lambda R X$  places the minimal HDOV truncation in the formal neighborhood of scalar-tensor theories with kinetic-geometric couplings (Horndeski, 1974; Kobayashi et al., 2011; Bellini and Sawicki, 2014). However, this observation should not be interpreted as a claim of full equivalence with a Horndeski theory. In the usual Horndeski notation, a sector of the form  $G_4(\Psi, X)R$  is accompanied, when  $G_4$  depends on  $X$ , by specific combinations of second derivatives of the scalar that cancel higher-order equations. Schematically, the relevant structure contains

$$G_4(\Psi, X)R + G_{4X} \left[ (\square \Psi)^2 - \nabla_\mu \nabla_\nu \Psi \nabla^\mu \nabla^\nu \Psi \right]. \quad (30)$$

The truncation used here retains the local operator  $\lambda R X$  as the minimal metric closure induced by  $\eta_p = \xi R$ , but it does not explicitly include the compensating term in Eq. (30). For this reason, the model should be understood as a perturbative low-energy EFT, valid under the conditions of Section 4.4, and not as a fully closed Horndeski completion in all branches.

This distinction also fixes the scope of the equations derived in this section. Equations (23)–(25) are the operative equations of the minimal truncation adopted here; the full classification of degrees of freedom, hyperbolicity, and stability requires either comparing this EFT with a higher-order scalar-tensor completion or deriving the quadratic action around the background of interest. That task is identified as part of the subsequent program and is not assumed to be solved in the present manuscript.

## 4.2 Homogeneous Cosmological Background and Rolling Branch

To connect the metric sector with a future self-consistent validation, it is useful to make the homogeneous branch explicit:

$$ds^2 = dt^2 - a(t)^2 d\vec{x}^2, \quad \Psi = \bar{\Psi}(t), \quad (31)$$

so that

$$X = \dot{\bar{\Psi}}^2, \quad R = 6(\dot{H} + 2H^2). \quad (32)$$

Equations (27)–(29) then constitute the homogeneous system of the scalar–gravitational sector in the absence of external cosmological fluids. In particular, the scalar equation can be written as

$$(1 + 2\lambda R)(\ddot{\bar{\Psi}} + 3H\dot{\bar{\Psi}}) + 2\lambda\dot{R}\dot{\bar{\Psi}} + m^2\bar{\Psi} = 0, \quad (33)$$

while the expansion history is determined by the modified Friedmann equations with  $X = \dot{\bar{\Psi}}^2$ .

In a slow-roll regime,

$$|\ddot{\bar{\Psi}}| \ll 3H|\dot{\bar{\Psi}}|, \quad \dot{\bar{\Psi}}^2 \ll m^2\bar{\Psi}^2, \quad |\lambda\dot{R}| \ll H|1 + 2\lambda R|, \quad (34)$$

Eq. (33) is approximated by

$$\left[3H(1 + 2\lambda R) + 2\lambda\dot{R}\right]\dot{\bar{\Psi}} + m^2\bar{\Psi} \simeq 0. \quad (35)$$

If, in addition,  $|\lambda|\dot{\bar{\Psi}}^2 \ll 1/\kappa$  and  $|\lambda H\dot{X}| \ll H^2/\kappa$ , the first Friedmann equation reduces to

$$3H^2 \simeq \kappa \frac{m^2\bar{\Psi}^2}{2} \left[1 + \mathcal{O}\left(\kappa\lambda\dot{\bar{\Psi}}^2, \frac{\lambda H\dot{X}}{H^2/\kappa}, \frac{\lambda R\dot{\bar{\Psi}}^2}{H^2/\kappa}\right)\right]. \quad (36)$$

These relations show that, at leading order, the rolling branch does not introduce a new kind of gravitational slip, but rather a controlled deformation of the FLRW background mediated by  $\lambda$ ,  $R$ , and the evolution of  $\bar{\Psi}(t)$ . A real cosmological comparison, however, cannot rely only on this idealized scalar branch: it must include matter, radiation, and their conservation laws. That minimal extension is introduced next.

These expressions do not yet close the PPN program or the full linear analysis, but they do explicitly incorporate the minimal metric sector needed to discuss HDOV as an effective theory of modified gravity.

## 4.3 Inclusion of Matter, Radiation, and Minimal Cosmological Closure

The homogeneous branch above describes the minimal scalar–gravitational sector, but it does not yet constitute a complete cosmological model. To compare the formalism with expansion data, at least non-relativistic matter and radiation must be included as minimally coupled perfect fluids. The extended starting point is

$$S_{\text{tot}} = S[g, \Psi] + S_m[g, \psi_m] + S_r[g, \psi_r], \quad (37)$$

where  $S_m$  and  $S_r$  represent the effective matter and radiation sectors. Since their couplings to the metric are minimal, their stress-energy tensors obey the usual covariant conservation equations in the FLRW background.

With the same conventions as in Eqs. (28) and (29), the extended background equations can be written as

$$3H^2 \left(\frac{1}{\kappa} + 2\lambda\dot{\bar{\Psi}}^2\right) = \rho_m + \rho_r + \rho_\Psi - 6\lambda H\dot{X} - 2\lambda R\dot{\bar{\Psi}}^2, \quad (38)$$

$$-(2\dot{H} + 3H^2) \left( \frac{1}{\kappa} + 2\lambda \dot{\Psi}^2 \right) = p_m + p_r + p_\Psi - 2\lambda(\ddot{X} + 2H\dot{X}), \quad (39)$$

with

$$\rho_\Psi = \frac{1}{2} \dot{\Psi}^2 + \frac{1}{2} m^2 \bar{\Psi}^2, \quad p_\Psi = \frac{1}{2} \dot{\Psi}^2 - \frac{1}{2} m^2 \bar{\Psi}^2, \quad X = \dot{\Psi}^2. \quad (40)$$

For cold matter and radiation we adopt

$$p_m \simeq 0, \quad p_r = \frac{1}{3} \rho_r, \quad (41)$$

and the conservation equations

$$\dot{\rho}_m + 3H\rho_m = 0, \quad \dot{\rho}_r + 4H\rho_r = 0. \quad (42)$$

In terms of redshift, with  $1 + z = a_0/a$ ,

$$\rho_m(z) = \rho_{m0}(1+z)^3, \quad \rho_r(z) = \rho_{r0}(1+z)^4. \quad (43)$$

The scalar-field dynamics remains

$$(1 + 2\lambda R)(\ddot{\Psi} + 3H\dot{\Psi}) + 2\lambda\dot{R}\dot{\Psi} + m^2\bar{\Psi} = 0, \quad (44)$$

with  $R = 6(\dot{H} + 2H^2)$  for a spatially flat background.

Thus, the minimal cosmological system is defined by Eqs. (38)–(44), together with the geometric definition of  $R$  and the conservation laws for matter and radiation. In practice, because  $\dot{R}$ ,  $\dot{X}$ , and  $\dot{\bar{X}}$  appear, this formulation should be treated as an effective differential-algebraic system, or rewritten with auxiliary variables before numerical integration. A natural set of evolution variables is

$$\mathcal{Y}(t) = \{H, \dot{H}, \bar{\Psi}, \dot{\Psi}, \rho_m, \rho_r\}, \quad (45)$$

subject to the modified Friedmann constraint.

It is important to stress that no density  $\rho_\Lambda$  nor a constant pressure term  $p_\Lambda = -\rho_\Lambda$  has been added in Eqs. (38)–(44). Therefore, the formulation allows one to study whether an accelerated expansion history can emerge from the geometric–functional HDOV sector. This, however, is not yet a demonstration of the absence of dark energy: such a claim would require solving the extended system, fitting  $H(z)$ , luminosity distances and BAO observables with full covariances, and statistically comparing with  $\Lambda$ CDM using  $\chi^2$ , AIC and BIC.

#### 4.4 EFT Conditions and Minimal Stability of the Truncation

The closure  $\eta_p = \xi R$  and the induced coupling  $\lambda R X$  must be interpreted as the first terms in an effective expansion in curvature and derivatives. The minimal model is therefore not intended to describe arbitrary-curvature regimes, but a perturbative domain in which higher-order corrections remain subdominant. In this version we adopt the necessary consistency conditions

$$|2\lambda R| \ll 1, \quad |2\kappa\lambda X| \ll 1, \quad \frac{|R|}{M^2} \ll 1, \quad (46)$$

where  $\lambda = g_c \xi$  and, if  $\xi = \alpha/M^2$ , the scale  $M$  represents the effective cutoff of the leading operator. The first condition controls the scalar kinetic correction, the second prevents the renormalization of the gravitational coupling from becoming non-perturbative, and the third expresses the hierarchy of the EFT expansion.

At the level of kinetic signs, the truncation requires that the multiplicative factor of the scalar equation does not change sign,

$$Z_\Psi \equiv 1 + 2\lambda R > 0, \quad (47)$$

and that the effective coefficient of the Einstein tensor in the metric equation remains positive,

$$M_{\text{eff}}^2 \equiv \frac{1}{\kappa} + 2\lambda X > 0. \quad (48)$$

Equation (47) is a necessary condition to avoid a sign flip of the effective scalar kinetic term in the background regime considered. Equation (48) prevents the effective gravitational coupling from crossing a coupling singularity. In particular, the slowly varying homogeneous branch gives

$$G_{\text{eff}} = \frac{G}{1 + 2\kappa\lambda X}, \quad (49)$$

so that  $1 + 2\kappa\lambda X > 0$  is a minimal regularity condition for the metric sector.

Gradient stability must not be assumed globally either. In the local limit where  $R$  varies slowly compared with the propagation scale of the scalar mode, the principal part of the equation for  $\Psi$  preserves the metric characteristic cone and the leading value is  $c_s^2 \simeq 1$ . However, when variations of  $R$  are rapid or when higher-order EFT terms are no longer negligible, corrections to propagation may arise and require a full perturbative analysis. We therefore impose, as operational conditions for using the truncation,

$$\frac{|\nabla_\mu R|}{|R|k} \ll 1, \quad \frac{|\Box R|}{M^2|R|} \ll 1, \quad |\lambda \nabla_\mu \nabla_\nu X| \ll \frac{1}{\kappa L^2}, \quad (50)$$

where  $k$  is the wavenumber scale of the mode considered and  $L$  the macroscopic scale of the background. These inequalities are not new dynamical equations, but control criteria ensuring that the local approximation and the leading truncation remain reliable.

In homogeneous cosmology, the previous conditions become practical constraints on the background evolution,

$$|2\lambda R| \ll 1, \quad |\lambda \dot{R}| \ll H|1 + 2\lambda R|, \quad |\kappa \lambda \dot{\Psi}^2| \ll 1, \quad (51)$$

under which Eqs. (38)–(44) can be used as a low-energy effective system. In strong gravity, or near regions where  $Z_\Psi$  or  $M_{\text{eff}}^2$  vanish, the minimal truncation should be considered insufficient and must be completed with higher operators or with the microscopic dynamics of the auxiliary sector.

**Table 2:** Minimal conditions for EFT validity and perturbative stability of the  $\lambda R X$  truncation. They are necessary conditions within the effective model, not a global proof of stability of all dynamical branches.

Criterion	Condition	Interpretation
EFT hierarchy	$ 2\lambda R  \ll 1,  R /M^2 \ll 1$	Higher-curvature corrections remain subdominant.
Metric coupling	$ 2\kappa\lambda X  \ll 1$	The renormalization of $G_{\text{eff}}$ remains perturbative.
Leading scalar no-ghost condition	$Z_\Psi = 1 + 2\lambda R > 0$	The effective kinetic term of $\Psi$ does not change sign.
Gravitational regularity	$M_{\text{eff}}^2 = 1/\kappa + 2\lambda X > 0$	The effective tensor-sector coefficient remains positive.
Derivative control	$ \lambda\nabla\nabla X $ small compared with the geometric scale	Mixing terms do not dominate the metric equation.
Cosmological validity	$ \lambda\dot{R}  \ll H 1 + 2\lambda R $	The FLRW branch can be treated as a slow evolution of the leading truncation.

These conditions delimit the domain in which the predictions of the paper should be interpreted. In particular, the PPN results of Section 5 and the cosmological benchmark of Section 6 rely on this perturbative regime. A complete stability proof would require the quadratic action for scalar, vector and tensor perturbations around general backgrounds, which is beyond the scope of the present version.

## 5 Linear Limit and Post-Newtonian Sector

To discuss the weak-field regime, we add a minimally coupled ordinary-matter sector,

$$S_{\text{tot}} = S[g, \Psi] + S_m[g, \psi_m], \quad (52)$$

and linearize around a locally nearly Minkowskian background,

$$g_{\mu\nu} = \eta_{\mu\nu} + h_{\mu\nu}, \quad \Psi = \bar{\Psi} + \varphi, \quad |h_{\mu\nu}| \ll 1. \quad (53)$$

We denote

$$X = \bar{X} + \delta X + \mathcal{O}(2), \quad \bar{X} \equiv \partial_\mu \bar{\Psi} \partial^\mu \bar{\Psi}. \quad (54)$$

The scalar equation linearized from Eq. (16) is

$$(1 + 2\lambda\bar{R})\square\varphi + m^2\varphi + 2\lambda(\partial_\mu\bar{R})\partial^\mu\varphi + 2\lambda(\partial_\mu\bar{R}^{(1)})\partial^\mu\bar{\Psi} = 0. \quad (55)$$

This equation shows an important point for the PPN regime: in the minimal action ordinary matter does not couple directly to  $\Psi$ . Hence, unlike in many scalar–tensor models, no linear baryonic scalar charge appears on the right-hand side of the equation for  $\varphi$ . Scalar excitations in the weak field must arise from boundary conditions, a non-trivial background  $\bar{\Psi}$ , residual cosmological gradients, or non-minimal extensions not included in the current truncation.

### 5.1 Post-Newtonian Counting and Local Vacuum Branch

We adopt the standard post-Newtonian counting for slow, quasi-static sources:  $v^2 \sim |\Phi| \sim \epsilon$ ,  $\partial_t = \mathcal{O}(v\partial_i)$ , internal pressures subdominant relative to mass density, and a metric written in Newtonian gauge,

$$ds^2 = (1 + 2\Phi)dt^2 - (1 - 2\Psi_N)\delta_{ij}dx^i dx^j. \quad (56)$$

In a local vacuum branch with

$$\bar{g}_{\mu\nu} = \eta_{\mu\nu}, \quad \bar{R} = 0, \quad \bar{\Psi} = 0, \quad (57)$$

Eq. (55) reduces to

$$\square\varphi + m^2\varphi = 0. \quad (58)$$

With boundary conditions excluding free incoming scalar modes, the solution  $\varphi = 0$  is consistent at first order in the presence of weak baryonic sources. In that branch,

$$X = \mathcal{O}(\varphi^2), \quad \delta X = \mathcal{O}(2), \quad T_{\mu\nu}^{(0,1)} = 0, \quad (59)$$

and Eq. (23) reduces to

$$G_{\mu\nu}^{(1)} = \kappa T_{\mu\nu}^{(m,1)}. \quad (60)$$

Therefore, the linear limit of the minimal metric sector coincides exactly with that of General Relativity in the local vacuum branch with  $\bar{\Psi} = 0$ .

In the gauge of Eq. (56), Eq. (60) implies

$$\nabla^2\Phi = 4\pi G\rho, \quad \Phi = \Psi_N. \quad (61)$$

Following the standard PPN parametrization (Will, 2014), equality of the potentials immediately gives

$$\gamma = 1. \quad (62)$$

Moreover, since in this branch the term  $\lambda R X$  starts at quadratic order in scalar perturbations, the post-Newtonian metric retains the Einstein–Hilbert structure and introduces no additional scalar nonlinearity at the order considered. Consequently,

$$\beta = 1 \quad (63)$$

in the minimal vacuum branch and under the specified boundary conditions. This conclusion should be read as a branch result: it does not prove that all solutions of the model have PPN parameters identical to GR, but identifies a local branch compatible with solar-system tests dominated by  $\gamma$  and  $\beta$ .

### 5.2 Slowly Varying Homogeneous Background and Effective Gravitational Constant

The previous result can be cautiously generalized to a slowly varying homogeneous background with  $\bar{X} \neq 0$  but approximately constant on Solar-System scales. Neglecting spatial derivatives of  $\delta X$  and terms proportional to  $\partial_i \bar{\Psi}$ , the linearized equation takes the form

$$\left(\frac{1}{\kappa} + 2\lambda\bar{X}\right) G_{\mu\nu}^{(1)} \simeq T_{\mu\nu}^{(m,1)}, \quad (64)$$

which yields the effective gravitational constant

$$G_{\text{eff}} = \frac{G}{1 + 2\kappa\lambda\bar{X}}. \quad (65)$$

As long as  $\bar{X}$  is locally homogeneous, the ratio between the potentials remains unity at first order, so that the gravitational slip remains zero and the leading value of  $\gamma$  is unchanged. If  $\bar{X}$  evolves cosmologically, the locally measured quantity should be interpreted as the renormalized Newton constant at the observational epoch. A necessary local compatibility condition is then that the temporal variation be sufficiently slow,

$$\left| \frac{\dot{G}_{\text{eff}}}{G_{\text{eff}}} \right| = \left| \frac{2\kappa\lambda\dot{\bar{X}}}{1 + 2\kappa\lambda\bar{X}} \right| \quad \text{small on Solar-System scales.} \quad (66)$$

This condition is not evaluated numerically in the present manuscript; it remains a requirement for a later comparison with observational bounds on temporal variation of  $G$ .

### 5.3 Possible Sources of PPN Deviations

The equality  $\Phi = \Psi_N$  obtained in the branches above can fail if the scalar background has spatial gradients, if  $\delta X$  develops local structure, or if additional non-minimal couplings between matter and  $\Psi$  are introduced. Schematically, corrections to the potentials take the form

$$\Phi - \Psi_N = \mathcal{O}\left(\lambda\partial_i\partial_j\delta X, \lambda R\partial_i\bar{\Psi}\partial_j\bar{\Psi}, \lambda\dot{\bar{X}}\right), \quad (67)$$

which identifies the assumptions required to recover the GR limit. In particular, a full PPN analysis of branches with  $\bar{\Psi} \neq 0$  and non-negligible gradients would require deriving the metric solution to complete post-Newtonian order, including vector potentials and the  $v^4$  terms in  $g_{00}$ . That task is beyond the scope of the present work.

Thus, the PPN sector of the minimal model can be summarized as

$$\gamma = 1 + \mathcal{O}(\partial_i\bar{\Psi}, \partial_i\partial_j\delta X, \dot{\bar{X}}), \quad \beta = 1 + \mathcal{O}(\partial_i\bar{\Psi}, \partial_i\partial_j\delta X, \dot{\bar{X}}), \quad (68)$$

with a possible renormalization of  $G$  given by Eq. (65). This result shows that the minimal metric truncation of HDOV contains a local branch compatible, at first order and under the stated assumptions, with solar-system constraints dominated by  $\gamma$  and  $\beta$ . It is not yet a general PPN proof of the model, and it leaves open the possibility of deviations in cosmological backgrounds or branches with a non-trivial scalar field.

**Table 3:** PPN sector of the minimal metric truncation of HDOV under the assumptions stated in Section 5.

Background branch	Local requirements	Leading result	Main limitation
Local vacuum ( $\bar{\Psi} = 0$ )	No free incoming scalar modes; minimally coupled matter	$G_{\text{eff}} = G$ , $\gamma = 1$ , $\beta = 1$	Valid only for the minimal vacuum branch
Homogeneous background, $\bar{X} \approx \text{const.}$	$\partial_i\bar{\Psi} \simeq 0$ , $\partial_i\delta X \simeq 0$ , small $ \dot{\bar{X}} $	$G_{\text{eff}} = G/(1 + 2\kappa\lambda\bar{X})$ , no leading slip	Requires control of temporal variation of $G_{\text{eff}}$
Background with scalar gradients	Non-negligible gradients or local structure in $\delta X$	Possible corrections to $\gamma$ and $\beta$	Requires a full PPN analysis of the inhomogeneous branch

## 5.4 Scope of the PPN Result

The central result of this section is negative in a technical sense: the minimal truncation does not automatically generate a baryonic fifth force or a linear gravitational slip in the local vacuum branch. This makes the minimal version compatible, at leading order, with the weak-field limit of GR. However, full compatibility with the PPN formalism still requires: (i) obtaining the metric solution through order  $v^4$ ; (ii) analyzing branches with  $\bar{\Psi} \neq 0$  and local gradients; (iii) confronting the time variation of  $G_{\text{eff}}$  with data; (iv) studying whether future extensions of the matter sector introduce effective scalar charges; and (v) calculating the complete set of PPN parameters, including possible preferred-frame or non-conservation parameters such as  $\alpha_1$ ,  $\alpha_2$ ,  $\alpha_3$  and  $\xi_{\text{PPN}}$ , if the branch considered allows them. The equalities  $\gamma = \beta = 1$  should therefore be understood as a property of the minimal branch, not as a universal demonstration over the full space of HDOV solutions.

## 6 Reproducible Phenomenological Benchmark with SN Ia and BAO

In this section we preserve the already reproducible observational work, but reframe it strictly as a phenomenological propagation benchmark. The analysis refers to Type Ia Supernovae as distance tracers in observational cosmology (Riess et al., 1998; Perlmutter et al., 1999; Scolnic et al., 2018) and to BAO measurements from SDSS DR16/eBOSS (Alam et al., 2021). Its purpose is not to demonstrate that the HDOV FLRW system already reproduces the data self-consistently, but to document that an effective parametric branch compatible with the geometric closure can generate curves, residuals and diagnostic metrics comparable with a reference model.

The methodological distinction is essential. Equations (38)–(44) define the minimal dynamical cosmological system associated with the coupling  $\lambda R X$ , including matter and radiation. By contrast, the figures and metrics in this section come from a previous phenomenological pipeline in which the effective modulation is introduced through a parametric propagation family, representable in terms of  $\eta_p(z)$  or of the derived visibility  $\mathcal{V}_p(z)$ . Therefore, the benchmark does not by itself prove that the same function is generated by a solution of the extended FLRW equations for some set of initial conditions and EFT parameters.

To avoid ambiguity, Table 4 summarizes the validation hierarchy used in this work. The table is placed before the figures because it fixes the meaning of the residuals and of the information criteria reported later.

**Table 4:** Hierarchy of cosmological validation considered for HDOV. The first row describes the benchmark implemented in this version: a reproducible phenomenological fit of propagation observables. The following rows identify the steps required to turn that benchmark into a dynamical validation of the full FLRW system. The table states what is demonstrated in the manuscript and what remains pending.

Level	Implemented in this version	Physical scope
Propagation benchmark	A finite effective parametric family compatible with HDOV is fitted to SN Ia and BAO; internal residuals, $\chi_{\text{eff}}^2$ , AIC and BIC are reported.	Reproducible diagnostic of phenomenological compatibility; not equivalent to solving the HDOV FLRW system.
Background validation	Pending: solve Eqs. (38)–(44) to obtain $H(z)$ from the dynamics.	Would allow $D_L(z)$ , BAO and $H(z)$ to be built from self-consistent solutions.
EFT control of the fit	Pending for the dynamical branch: verify $ 2\lambda R  \ll 1$ , $Z_\Psi > 0$ and $M_{\text{eff}}^2 > 0$ over the redshift range.	Determines whether the fit remains within the EFT validity domain.
Perturbations	Not included.	Requires structure growth, CMB/lensing and linear stability.

## 6.1 Operational Definition of the Benchmark

The benchmark uses the Type Ia Supernova sample to construct an effective distance modulus and uses BAO as additional constraints in the joint fit. Operationally, the standardized apparent magnitude is converted into a distance modulus through the absolute-magnitude calibration of the pipeline,

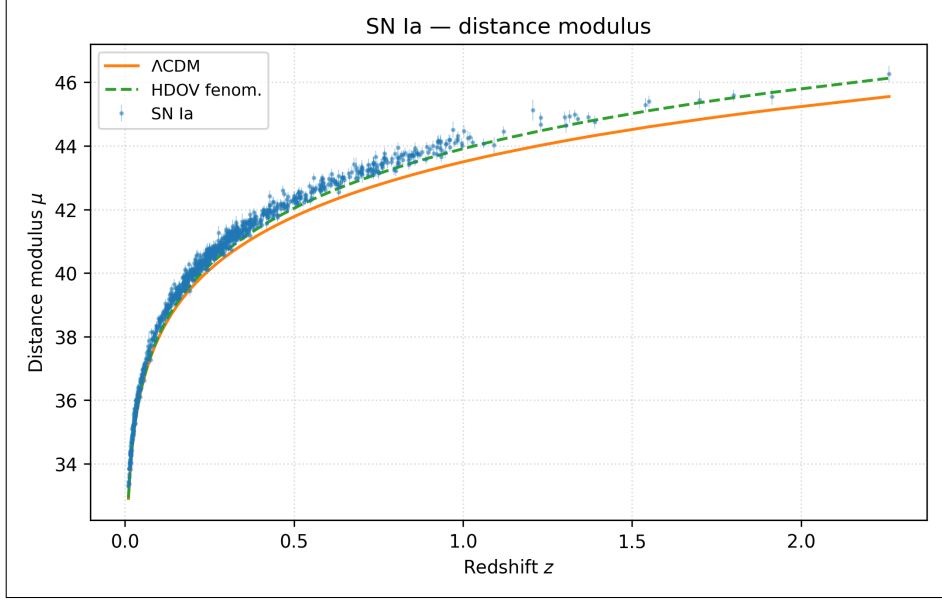
$$\mu_{\text{obs}} = m_B - M_B, \quad (69)$$

and the model curves are compared with  $\mu_{\text{obs}}(z)$  within the same normalization. The phenomenological HDOV branch does not introduce an arbitrary point-by-point free function: it is restricted to a finite parametric family in the pipeline. Even so, because that family is not yet obtained by solving Eqs. (38)–(44), the effective parameters in Table 5 should not be directly identified with a unique pair  $(\lambda, \xi)$  or with initial conditions of the metric theory.

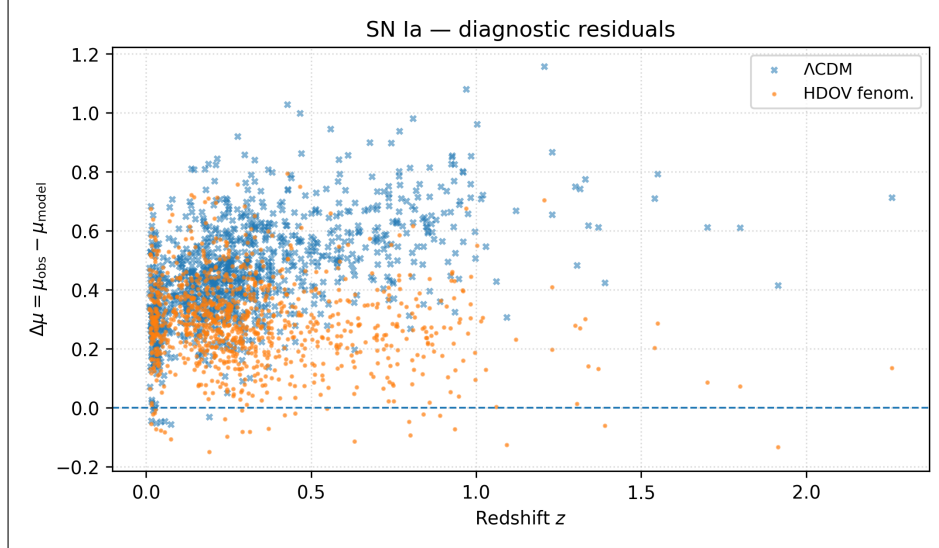
This clarification addresses an important limitation: the EFT conditions in Section 4.4 can be checked unambiguously only when the best fit comes from a dynamical solution with determined  $R(z)$ ,  $X(z)$  and  $\Psi(z)$ . In the current benchmark, those conditions remain requirements for the future self-consistent version, not already closed checks of the phenomenological curves.

## 6.2 Phenomenological Figures and Residuals

Figures 2 and 3 show curves and residuals obtained in the reproducible phenomenological scheme. Figure 2 summarizes the diagnostic comparison based on Type Ia Supernovae, while Fig. 3 shows the distance-modulus projection obtained when using the parameters of the combined SN+BAO phenomenological fit. In the latter figure, BAO observables are not plotted as distance-modulus points; they enter as parametric constraints within the joint fit. Within this benchmark, the phenomenological HDOV branch is visually closer to the SN cloud and has lower-amplitude residuals than the  $\Lambda$ CDM reference curve used in the same pipeline. This observation should be read as an internal diagnostic of the effective parametrization, not as a definitive cosmological model-selection result.

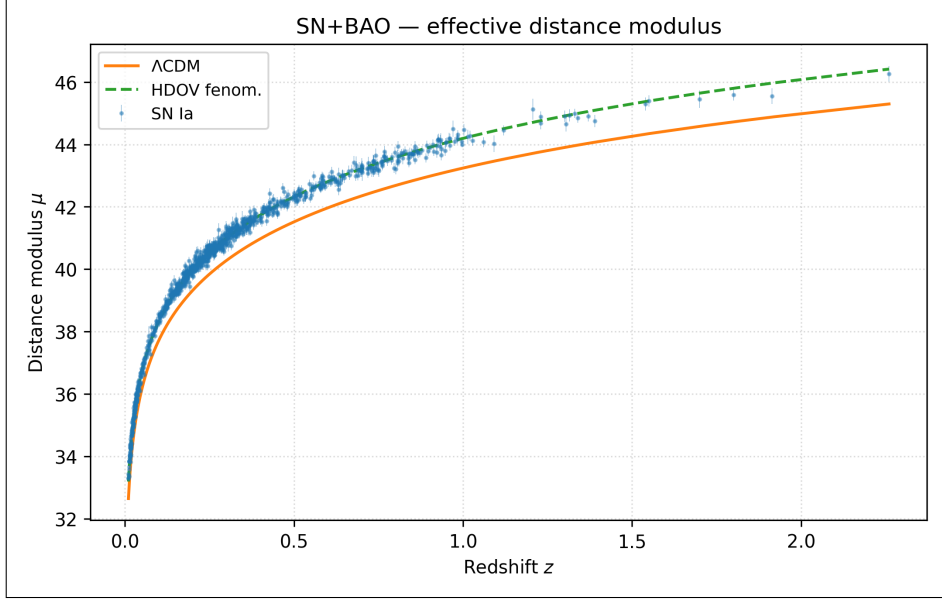


(a) Distance-modulus projection for the Type Ia Supernova sample used in the reproducible pipeline. The horizontal axis is redshift and the vertical axis is the effective distance modulus defined in Eq. (69). The points correspond to the supernova sample and the curves to the models indicated in the figure legend.

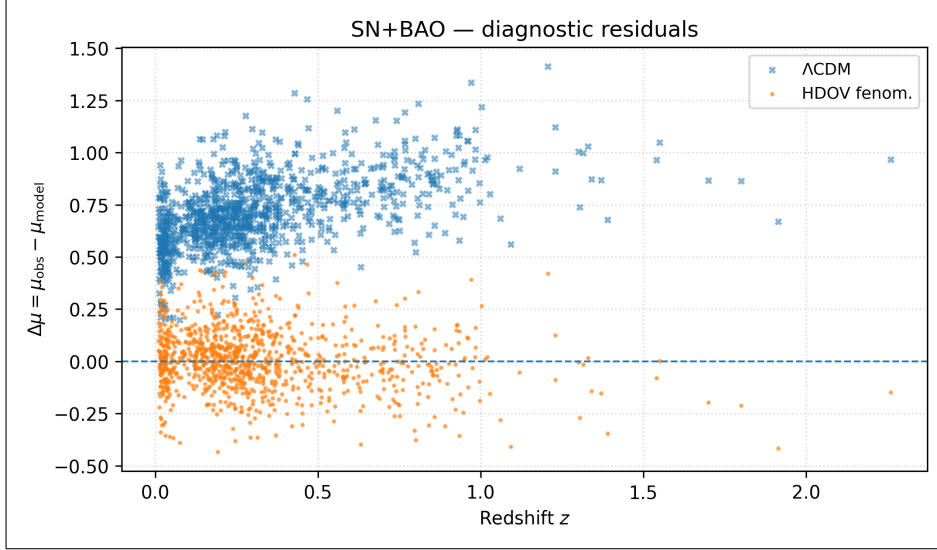


(b) Residuals associated with the previous panel. The horizontal axis is redshift and the vertical axis is the difference between the observed distance modulus and the distance modulus of the model indicated in the legend. The horizontal line marks zero residual. The lower residual amplitude of the HDOV branch in this panel is a property of the phenomenological benchmark and does not replace a self-consistent FLRW fit.

**Figure 2:** Phenomenological benchmark for the Type Ia Supernova analysis. The upper panel shows observational SN points and model curves indicated in the legend; the lower panel shows residuals relative to those curves and the zero-residual line. In this diagnostic output, the phenomenological HDOV branch has smaller residuals than the  $\Lambda$ CDM reference curve within the same pipeline; this comparison does not yet constitute a definitive cosmological validation of the minimal metric system.



(a) Distance-modulus projection for the Type Ia Supernova sample using the parameters obtained in the combined SN+BAO phenomenological fit. The horizontal axis is redshift and the vertical axis is the effective distance modulus. The points correspond to the projected SN sample; BAO observables are not represented here as distance-modulus points, but are incorporated as additional constraints of the joint pipeline.



(b) Residuals of the SN projection obtained with parameters from the combined SN+BAO phenomenological fit. The horizontal axis is redshift and the vertical axis is the difference between the observed distance modulus and that of the model indicated in the legend. The horizontal line marks zero residual. The visually closer approach of the HDOV branch to zero residual is interpreted as a diagnostic result of the benchmark, not as a direct representation of BAO observables.

**Figure 3:** Phenomenological distance-modulus benchmark using parameters from the combined SN+BAO analysis. The upper panel shows the projected SN sample and the model curves indicated in the legend; the lower panel shows the corresponding residuals and the zero-residual line. BAO data enter as constraints of the joint fit, not as distance-modulus points in this figure. Within the pipeline used here, the HDOV branch has more centered residuals than the  $\Lambda$ CDM reference; the comparison remains preliminary because it does not follow from solving the full metric equations.

### 6.3 Effective Expansion History and Interpretation of the Closure

In the proposed minimal closure,  $\eta_p = \xi R$ , the relevant variable is not a freely reconstructed function but a geometric magnitude induced by the scalar curvature. In the current benchmark, however, the fitted object should be understood as an effective representation of  $\xi R(z)$  within a propagation scheme, not as the complete cosmological solution of the HDOV metric system. Figure 4 is retained with this strictly illustrative status.

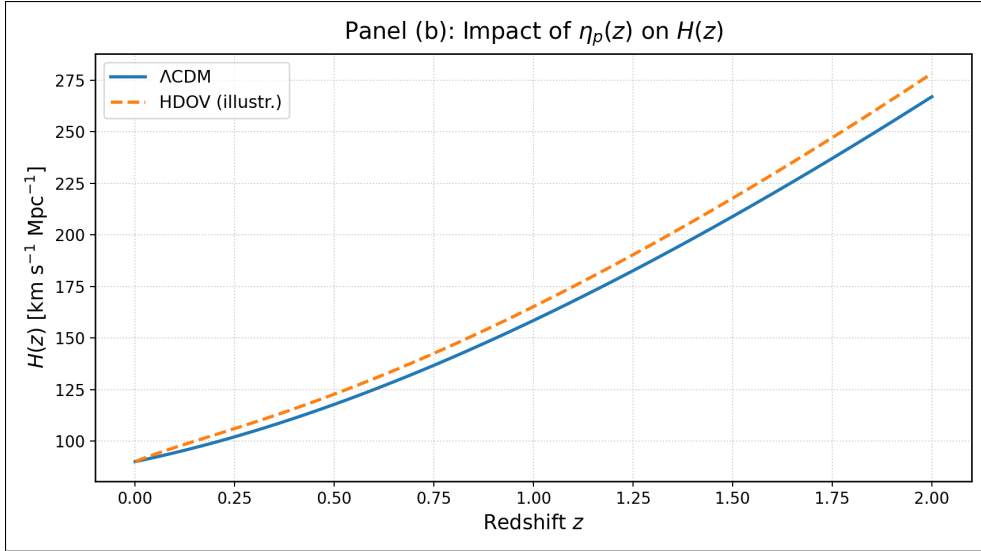


**Figure 4:** Illustrative comparison of the effective expansion history in the phenomenological benchmark. The horizontal axis is redshift and the vertical axis is the expansion rate in units of  $\text{km s}^{-1} \text{Mpc}^{-1}$ . The solid line shows the  $\Lambda\text{CDM}$  reference model and the dashed line the effective branch compatible with HDOV used in the pipeline. The figure does not replace the self-consistent integration of the extended FLRW system and does not by itself fix the EFT parameters of the metric coupling.

### 6.4 Diagnostic Metrics and Statistical Scope

For a comparison between HDOV and  $\Lambda\text{CDM}$  to be publishable as a complete cosmological test, the statistical metrics must be computed from a likelihood with observational covariances, nuisance parameters, and a prediction  $H(z)$  derived from the background equations. For Type Ia Supernovae, this implies separating the distance modulus from the absolute-magnitude calibration, including the covariance matrix, and comparing with modern catalogs such as Pantheon+ (Scolnic et al., 2022; Brout et al., 2022). For BAO, a later stage should include, in addition to SDSS DR16, DESI DR1 measurements with transverse and radial distances in redshift bins (DESI Collaboration et al., 2025a,b).

The reproducibility package retains a diagnostic output of the phenomenological pipeline, summarized in Table 5. We define here  $\chi_{\text{eff}}^2 \equiv -2 \ln \mathcal{L}_{\text{tot}}$  only as an internal indicator of the benchmark. The information criteria are

$$\text{AIC} = 2k - 2 \ln \hat{\mathcal{L}}, \quad \text{BIC} = k \ln N - 2 \ln \hat{\mathcal{L}}, \quad (70)$$

where  $k$  is the number of effective parameters,  $N$  the number of data points, and  $\hat{\mathcal{L}}$  the maximum likelihood (Akaike, 1974; Schwarz, 1978; Kass and Raftery, 1995). In Table 5,  $k$  counts only the explicit free parameters of the implemented parametric family. It does not include a non-parametric functional penalty because the benchmark does not fit  $\eta_p(z)$  point by point; even so, this convention prevents using  $\Delta\text{BIC}$  as final model-selection evidence.

**Table 5:** Diagnostic metrics of the reproducible phenomenological benchmark. Each row lists the model compared, the number of data points, the effective number of explicit parameters, and the AIC/BIC criteria defined in Eq. (70); the BIC-difference column is measured with respect to the reference model. Within this benchmark, the HDOV branch obtains lower values of  $\chi^2_{\text{eff}}$ , AIC and BIC than the  $\Lambda$ CDM reference. This advantage is diagnostic of the pipeline and must be recalculated in a self-consistent stage with full covariances, the same treatment of nuisance parameters, and  $H(z)$  derived from the background equations.

Model	$\chi^2_{\text{eff}}$	$N$	$k$	AIC	BIC	$\Delta\text{BIC}$
Phenomenological HDOV	1062.3	1071	5	1072.3	1097.2	-10.48
$\Lambda$ CDM reference	1065.8	1071	6	1077.8	1107.7	0.00

The cautious reading of Table 5 is the following: the current scheme produces an auditable numerical output and, within its own parametric family, favors the phenomenological HDOV branch over the  $\Lambda$ CDM reference. However, the statistical interpretation remains conditioned by SN/BAO normalization, the inclusion of full covariances, the correct penalization of effective functional freedom, and the derivation of  $H(z)$  from the extended HDOV system. These values are therefore reported as a reproducibility diagnostic, not as conclusive evidence for replacing  $\Lambda$ CDM or eliminating dark energy.

**Table 6:** Observational status of the HDOV cosmological branch. The first column identifies the data block or physical test, the second summarizes what is implemented in this version, and the third states the minimal technical requirement for a strict cosmological-validation stage. The table separates the reproducible phenomenological benchmark from the still pending program of self-consistent dynamical fitting.

Observational block	Status in this version	Requirement for a publishable stage
SN Ia	Phenomenological benchmark with Pantheon	Reprocess observable, absolute magnitude, covariance and nuisance parameters; migrate to Pantheon+
BAO	Preliminary constraints with SDSS DR16/eBOSS	Include BAO covariances and compare with DESI DR1
$H(z)$	Illustrative effective curve	Obtain $H(z)$ by solving the extended FLRW equations
AIC/BIC	Diagnostic output of the pipeline	Recompute with full likelihood, same data and same nuisance treatment
EFT control	Not unambiguously verifiable for the benchmark	Evaluate $ 2\lambda R $ , $Z_\Psi$ and $M_{\text{eff}}^2$ on the fitted dynamical solution
Perturbations	Not included	Add structure growth, CMB/lensing and linear stability

Consequently, this section preserves the value of the data and reproducibility work, but locates it at the appropriate epistemic level. The necessary stage for a strong cosmological claim will be to solve numerically the extended system in Eqs. (38)–(44), obtain  $H(z)$  directly from the dynamical equations, and recompute  $\chi^2$ , AIC and BIC with homogeneous observables and covariances.

## 7 Discussion and Conclusions

In this revision we have closed the minimal gravitational sector of HDOV through the effective coupling  $\lambda RX$ , obtaining a scalar equation, an explicit metric response, its trace equation, and the corresponding FLRW background system. This step allows HDOV, in its minimal version, to be presented as a better-defined effective proposal for modified gravity than in previous versions. At the same time, we have explicitly separated the derived dynamical system from the phenomenological benchmark used to inspect SN Ia and BAO data. The manuscript should therefore be read as a technically stronger formulation of the gravitational sector and as a basis for future complete fits, not as a definitive observational validation or as a demonstration that  $\Lambda$ CDM has been replaced.

### 7.1 HDOV in the Context of Other Theoretical Models

From a formal point of view, the minimal HDOV truncation belongs to the broad family of scalar–tensor theories with couplings between a scalar and curvature, although its conceptual starting point is different: the primary object of the model is the projective wave equation and the operational interpretation of accessibility, not a post hoc modification of the cosmological sector. In particular, the term  $\lambda RX$  places it near known classes of theories with kinetic–geometric couplings (Horndeski, 1974; Kobayashi et al., 2011; Bellini and Sawicki, 2014). As explained in Section 4.1, this proximity does not amount to a complete Horndeski completion: in the present work  $\lambda RX$  is used as a leading EFT operator associated with the closure  $\eta_p = \xi R$ , not as an exhaustive classification of all degrees of freedom of the model.

**Table 7:** Conceptual location of the minimal HDOV truncation relative to known scalar models. The table compares the characteristic term, the expected order of the equations in the regime considered, and the physical scope of each case. The HDOV row should be read as a perturbative EFT truncation induced by the adopted geometric closure, not as a complete classification of all dynamical branches.

Model	Characteristic term	Equation order	Comment
Minimal scalar	$X - m^2 \Psi^2$	second	baseline without geometric coupling
Standard non-minimal scalar	$F(\Psi)R$	second	Brans–Dicke/Jordan type, as a classical scalar–tensor reference (Brans and Dicke, 1961)
Minimal HDOV	$\lambda RX$	perturbative EFT	geometric kinetic modulation valid under the conditions of Table 2

At the phenomenological level, HDOV also differs from other frequently cited frameworks:

- **Gravity’s Rainbow:** postulates an energy-dependent metric, with possible effective deformation or breaking of the Lorentz structure (Magueijo and Smolin, 2004). In the truncation used here, HDOV keeps a local curvature-dependent closure and preserves covariance.
- **Stochastic Gravity:** introduces stochastic metric fluctuations and noise terms associated with quantum correlations of matter (Hu and Verdaguer, 2004). HDOV is deterministic in its minimal core, where inaccessibility is represented as functional modulation rather than as random noise.
- **Models of gravitational decoherence:** HDOV can be read as an effective parametrization inspired by decoherence or dynamical-reduction programs (Bassi and Ghirardi, 2003), but with an explicit functional-projection mechanism through  $\eta_p$ .

The main distinction of the present approach is therefore the geometric modulation of functional accessibility through a minimal covariant closure. In this version we avoid interpreting that closure as a fully established duality with analogue systems or as an already exhaustively classified scalar–tensor theory; such extensions require further microscopic and dynamical analysis.

## 7.2 Regime of Effective Validity and Consistency

The conclusions of the minimal truncation must be understood within the perturbative EFT regime defined in Section 4.4. In particular, the manuscript does not yet establish the complete degree-of-freedom structure of the model nor definitively exclude ghost or gradient instabilities outside that domain. The conditions  $|2\lambda R| \ll 1$ ,  $Z_\Psi = 1 + 2\lambda R > 0$  and  $M_{\text{eff}}^2 = 1/\kappa + 2\lambda X > 0$  should be read as necessary requirements for using the minimal version, not as a global stability proof. This version does not yet develop a full Hamiltonian analysis or derive the quadratic perturbation action around general backgrounds. The results presented are therefore restricted to weak fields, moderate curvatures and slowly varying backgrounds where the closure  $\eta_p = \xi R$  can be treated as a controlled low-energy truncation.

## 7.3 Limitations and Future Directions

Future work includes: (i) numerically solving the extended cosmological system in Eqs. (38)–(44) to generate a self-consistent  $H(z)$  in the presence of matter and radiation; (ii) verifying on that solution the EFT conditions  $|2\lambda R| \ll 1$ ,  $Z_\Psi > 0$  and  $M_{\text{eff}}^2 > 0$ ; (iii) deriving the quadratic action for scalar, vector and tensor perturbations to turn the necessary conditions in Table 2 into complete dynamical criteria; (iv) extending the PPN analysis beyond the minimal homogeneous branch, including non-trivial gradients, time variation of  $G_{\text{eff}}$  and possible effective scalar sources; (v) obtaining black-hole solutions and their perturbations for a serious quasi-normal-mode analysis; (vi) recomputing  $\chi^2$ , AIC and BIC with a complete likelihood and observational covariances; and (vii) complementing cosmological phenomenology with confidence intervals, growth-of-structure perturbations, CMB and lensing.

These tasks delimit the actual scope of the present article. In particular, the manuscript does not yet demonstrate the absence of dark energy, does not rule out singularities in general, and does not replace  $\Lambda$ CDM as the standard cosmological model; rather, it formulates an effective branch that can be subjected to mathematical and observational tests in later stages.

## 7.4 Predictions and Falsifiability Criteria in the Regime Considered

The minimal truncation suggests concrete falsifiability criteria once the full metric system has been closed and the initial conditions of each branch fixed:

- **Cosmology:** possible modifications in the expansion history and luminosity distances once the extended system with matter and radiation is solved self-consistently.
- **Weak-field regime:** in the minimal vacuum branch, the PPN sector coincides with GR at first order, with  $\gamma = \beta = 1$  and no linear baryonic fifth force. In branches with a non-trivial homogeneous background, the relevant prediction is a possible slow renormalization of  $G_{\text{eff}}$ ; local scalar gradients could generate deviations in  $\gamma$ ,  $\beta$  or gravitational slip.
- **Strong gravity:** possible shifts in quasi-normal modes only after obtaining black-hole solutions and their linear perturbations inside the complete metric sector.

The falsification of any of these blocks will depend on observables constructed from solutions of the dynamical system, not only from propagation parametrizations. The predictions above are therefore presented as a verifiable program, not as already established results.

## A EFT Motivation for the Minimal Closure

An example of how a non-local term can motivate a curvature-dependent  $\eta_p$  is the schematic effective action

$$S_{\text{nonlocal}} \sim \int d^4x \sqrt{-g} \frac{1}{M^2} R f(\square^{-1} R), \quad (71)$$

where  $f$  is analytic. Expanding  $f(x) = \alpha x + \beta x^2 + \dots$  gives, at leading order,

$$\eta_p \sim \frac{\alpha}{M^2} R + \mathcal{O}(R^2), \quad (72)$$

i.e. a curvature-dependent functional coupling. This argument does not replace a complete microscopic derivation; it only motivates using the leading closure  $\eta_p = \xi R$  as a minimal local EFT ansatz. The choice is not unique and does not exclude higher-curvature operators or additional non-local terms.

The validity of this motivation is restricted to the regime where derivatives and higher powers of curvature remain subdominant. Equations (71) and (72) should therefore be read as a truncation guide, not as a unique reconstruction of the microscopic sector.

## B Sketch of the Metric Variation of the Geometric Coupling

For the action

$$S_\lambda = \int d^4x \sqrt{-g} \lambda R X, \quad X \equiv \nabla_\mu \Psi \nabla^\mu \Psi, \quad (73)$$

the variation with respect to  $g^{\mu\nu}$  can be organized using

$$\delta X = \nabla_\mu \Psi \nabla_\nu \Psi \delta g^{\mu\nu}, \quad (74)$$

$$\delta(\sqrt{-g} R) = \sqrt{-g} [G_{\mu\nu} \delta g^{\mu\nu} + (g_{\mu\nu} \square - \nabla_\mu \nabla_\nu) \delta g^{\mu\nu}]. \quad (75)$$

Multiplying the second identity by  $X$  and integrating the boundary terms by parts gives

$$\delta S_\lambda = \int d^4x \sqrt{-g} \lambda [X G_{\mu\nu} + (g_{\mu\nu} \square - \nabla_\mu \nabla_\nu) X + R \nabla_\mu \Psi \nabla_\nu \Psi] \delta g^{\mu\nu} \quad (76)$$

$$\equiv \int d^4x \sqrt{-g} \lambda \mathcal{A}_{\mu\nu}^{(\lambda)} \delta g^{\mu\nu}, \quad (77)$$

where

$$\mathcal{A}_{\mu\nu}^{(\lambda)} = X G_{\mu\nu} + (g_{\mu\nu} \square - \nabla_\mu \nabla_\nu) X + R \nabla_\mu \Psi \nabla_\nu \Psi. \quad (78)$$

With the sign convention adopted in the text, the effective contribution of this term to the right-hand side of the metric equations is  $-2\lambda \mathcal{A}_{\mu\nu}^{(\lambda)}$ . Therefore,

$$\frac{1}{\kappa} G_{\mu\nu} = T_{\mu\nu}^{(0)} - 2\lambda \mathcal{A}_{\mu\nu}^{(\lambda)}, \quad (79)$$

and, after moving  $-2\lambda X G_{\mu\nu}$  to the left-hand side, Eq. (23) is recovered. This appendix does not replace a full Horndeski or  $f(R, X)$ -style derivation, but it makes explicit the functional step between the action and the field equations used in the manuscript.

## Data and Code Availability

All data used in the phenomenological section of this work, including the Pantheon catalog (Scolnic et al., 2018) and SDSS DR16 BAO measurements (Alam et al., 2021), are publicly available or distributed as derived files within the reproducibility package, according to the usage conditions of each source.

All source code used in this work is distributed with the reproducibility package `HDOV_repro_V6`, in the directories `src/core_fig/`. These include the scripts needed to reproduce the cosmological fits, the SN Ia and BAO figures, and the metrics associated with the phenomenological analysis described in this manuscript. The file `README_HDOV_repro.md` describes the package structure, the recommended Python environment and the basic execution instructions.

## Declarations and Contributions

**Conflict of interest:** The author declares that there is no financial or personal conflict of interest that could have influenced the results presented.

**Author contributions:** Arnaldo Fernández conceived the HDOV hypothesis, developed the mathematical formalism, performed the numerical analyses and wrote the manuscript.

**ORCID:** [0000-0003-3027-0450](https://orcid.org/0000-0003-3027-0450).

## References

- Akaike, H. (1974). A new look at the statistical model identification. *IEEE Transactions on Automatic Control*, 19(6):716–723.
- Alam, S., Aubert, M., Avila, S., Balland, C., Bautista, J. E., Bershady, M. A., Blanton, M. R., Bolton, A. S., Brownstein, J. R., Burtin, E., Chapman, M. J., Chuang, C.-H., Comparat, J., Dawson, K. S., de la Macorra, A., de Mattia, A., du Mas des Bourboux, H., Escoffier, S., Fernandez-Trincado, J. G., Font-Ribera, A., Frinchaboy, P. M., Gil-Marín, H., Gonzalez-Morales, A. X., Hawken, A. J., Hou, J., Jimenez, R., Kamiya, Y., Kneib, J.-P., Kong, H., Landy, S. D., Lang, D., Laurent, P., Le Goff, J.-M., Li, C., Lin, S., Lyke, B. W., Macpherson, H. J., Mohammad, F. G., Moustakas, J., Mueller, E.-M., Myers, A. D., Nadathur, S., Neveux, R., Newman, J. A., Ntelis, P., O’Connell, R., Oravetz, D. J., Oravetz, A., Palanque-Delabrouille, N., Percival, W. J., Pieri, M. M., Prakash, A., Raichoor, A., Rezaie, M., Ross, A. J., Rossi, G., Ruhlmann-Kleider, V., Sanchez, F., Sanchez, A. G., Schlegel, D. J., Schneider, D. P., Seo, H.-J., Shao, L., Smith, R. E., Tamone, A., Tinker, J. L., Tojeiro, R., Vargas-Maga a, M., Vivek, M., Wang, Y., Y’èche, C., and Zhao, G.-B. (2021). The completed SDSS-IV extended Baryon Oscillation Spectroscopic Survey: Cosmological implications from two decades of spectroscopic surveys at the Apache Point Observatory. *Phys. Rev. D*, 103(8):083533.
- Almheiri, A., Marolf, D., Polchinski, J., and Sully, J. (2013). Black holes: Complementarity or firewalls? *JHEP*, 2013(2):62.
- Bassi, A. and Ghirardi, G. (2003). Dynamical reduction models. *Phys. Rep.*, 379(5-6):257–426.
- Bellini, E. and Sawicki, I. (2014). Maximal freedom at minimum cost: linear large-scale structure in general modifications of gravity. *Journal of Cosmology and Astroparticle Physics*, 2014(07):050.
- Birrell, N. D. and Davies, P. C. W. (1982). *Quantum Fields in Curved Space*. Cambridge University Press.
- Brans, C. and Dicke, R. H. (1961). Mach’s principle and a relativistic theory of gravitation. *Physical Review*, 124(3):925–935.
- Brout, D., Scolnic, D., Popovic, B., Riess, A. G., Zuntz, J., Kessler, R., Carr, A., Davis, T. M., Hinton, S., Jones, D., et al. (2022). The pantheon+ analysis: Cosmological constraints. *The Astrophysical Journal*, 938(2):110.

- DESI Collaboration, Adame, A. G., Aguilar, J., Ahlen, S., Alam, S., Alexander, D. M., et al. (2025a). DESI 2024 iii: Baryon acoustic oscillations from galaxies and quasars. *Journal of Cosmology and Astroparticle Physics*, 2025(04):012.
- DESI Collaboration, Adame, A. G., Aguilar, J., Ahlen, S., Alam, S., Alexander, D. M., et al. (2025b). DESI 2024 vi: Cosmological constraints from the measurements of baryon acoustic oscillations. *Journal of Cosmology and Astroparticle Physics*, 2025(02):021.
- Horndeski, G. W. (1974). Second-order scalar-tensor field equations in a four-dimensional space. *International Journal of Theoretical Physics*, 10(6):363–384.
- Hu, B.-L. and Verdaguer, E. (2004). Stochastic gravity: theory and applications. *Living Reviews in Relativity*, 7(3).
- Kass, R. E. and Raftery, A. E. (1995). Bayes factors. *Journal of the American Statistical Association*, 90(430):773–795.
- Kobayashi, T., Yamaguchi, M., and Yokoyama, J. (2011). Generalized g-inflation: Inflation with the most general second-order field equations. *Progress of Theoretical Physics*, 126(3):511–529.
- Magueijo, J. and Smolin, L. (2004). Gravity’s rainbow. *Classical and Quantum Gravity*, 21(7):1725–1736.
- Parker, L. E. and Toms, D. J. (2009). *Quantum Field Theory in Curved Spacetime: Quantized Fields and Gravity*. Cambridge University Press.
- Perlmutter, S. et al. (1999). Measurements of omega and lambda from 42 high-redshift supernovae. *Astrophys. J.*, 517(2):565–586.
- Riess, A. G. et al. (1998). Observational evidence from supernovae for an accelerating universe and a cosmological constant. *Astron. J.*, 116(3):1009–1038.
- Schwarz, G. (1978). Estimating the dimension of a model. *The Annals of Statistics*, 6(2):461–464.
- Scolnic, D., Brout, D., Carr, A., Riess, A. G., Davis, T. M., Dwomoh, A., Jones, D. O., Ali, N., Charvu, P., Chen, R., et al. (2022). The pantheon+ analysis: The full data set and light-curve release. *The Astrophysical Journal*, 938(2):113.
- Scolnic, D. M., Jones, D. O., Rest, A., Pan, Y. C., Chornock, R., Foley, R. J., Huber, M. E., Kessler, R., Narayan, G., Riess, A. G., et al. (2018). The complete light-curve sample of spectroscopically confirmed sne ia from pan-starrs1 and cosmological constraints from the combined pantheon sample. *The Astrophysical Journal*, 859(2):101.
- Will, C. M. (2014). *Theory and Experiment in Gravitational Physics*. Cambridge University Press, Cambridge, 2 edition.